Effect of organoclay loading on the dielectric properties and charge dynamics of a PP-rubber nanocomposite

Allison V. Shaw[1], Phichet Ketsamee[1], Thomas Andritsch[1] ✉, Alun S. Vaughan[1]

[1]*Tony Davis High Voltage Laboratory, University of Southampton, UK*
✉ *E-mail: t.andritsch@soton.ac.uk*

Abstract: The addition of organoclay to a polypropylene-rubber (PP-rubber) blend, primarily introduced to compatibilise the immiscible polymer blend, invokes contrasting dielectric and charge dynamic behaviour depending on the filler loading level. The authors report that at 0.5 wt.% loading, the organoclay decreases the DC conductivity, causes no significant dielectric losses, makes no significant difference to the space charge results compared to the unfilled system, and increases the reproducibility of the breakdown strength results, and hence the reliability of the material. These somewhat surprising results, contrasted by measurements of samples with 2.5 and 5 wt.%, lead us to conclude that trace amounts of organoclay improve the otherwise immiscible polymer blend making organoclay a suitable additive for HVDC applications.

1 Introduction

Polypropylene (PP) is one of the most widely used non-polar polymers, in part due to its excellent insulating properties [1], while a mixture of polymers can be used to create a material exhibiting properties from both. For example, PP-rubber blends and PP-nanofiller composites have been investigated as a means to alter the mechanical properties of PP, specifically, to decrease the brittleness of PP [2, 3].

A recent publication on a PP-rubber blend containing an organically modified montmorillonite clay (organoclay) showed that the organoclay altered the dielectric properties of the immiscible blend [4]. Elsewhere, the dielectric properties of both PP and copolymer ethylene vinyl acetate (EVA) have been investigated thoroughly. Separately, both are used extensively for electrical insulation including for cables and capacitors [5]. PP is an attractive option since it is cheap, easy to process and has high corrosion resistance. On the other hand, EVA is known for elasticity and optical clarity, yet has a higher permittivity and lower melting point than PP [6]. To achieve a compromise between these properties, a blend of PP and EVA has seen literature attention for over 20 years. However, due to the difference in polarities, the polymers are incompatible and will phase separate without a compatibilising agent [7]. Tackling the phase separation of the polymers by removing the polar EVA is not feasible as the polar nature of EVA is essential to make the polymer matrix compatible with the organoclay [8]. Of course, where one does not require the addition of organoclay or EVA specifically, then using an alternative polymer blend is an option.

Many studies have considered using various types of organoclay as a compatibiliser and investigated the thermal and thermo-oxidative properties [9], mechanical properties [10] and gas barrier properties [11]. Elsewhere, the effects of organoclay on the dielectric properties such as conductivity, breakdown strength (BDS) and space charge of PP-organoclay and EVA-organoclay composites have been investigated [5]. In light of the literature leaving a distinct gap in the dielectric properties of PP-EVA blends compatibilised by organoclay, we previously undertook work that has been published elsewhere [12]. However, the achievement of compatibility for the polymer blend was somewhat overshadowed by the detrimental effects that the addition of organoclay had on the dielectric properties of the composites. Namely, the organoclay increasing the DC conductivity and decreased the DC dielectric BDS. Herein, we investigate whether the organoclay loading can be reduced to minimise the impact on the dielectric properties whilst retaining the ability to compatibilise the polymer blend.

Furthermore, this paper will also consider the space charge properties of the composites.

2 Experimental

Samples were produced following a solution blending technique. The organoclay was first sonicated in xylene for 20 min before being added, with the polymer pellets, to a rotary evaporator at 150°C and stirred until dissolution, whereupon the xylene was removed under vacuum and the product was dried under dynamic vacuum at 70°C for a week. Samples were produced using the PP and the organoclay, as received from Sigma Aldrich (product codes 427888 and 682624, respectively); the EVA, which contains 9 wt. % VA, was used as received from DuPont (Elvax750). The ratio of PP:EVA was always 80:20 and samples were made with either 0, 0.5, 2.5 or 5 wt. % of organoclay. All the samples were pressed at 180°C into films and then quenched from the melt phase in the air. The samples will be referred to as PP/EVA/X, where X represents the organoclay loading.

Internal cross-sections of samples were imaged, following an etching procedure [13], by scanning electron microscopy (SEM: EVO LS25, produced by Zeiss).

Dielectric spectra were acquired using a Solartron 1296 dielectric interface together with a Schlumberger SI1260 impedance/phase gain analyser system. An AC voltage of amplitude 1 V_{rms} was applied across a guarded electrode of diameter 30 mm; a frequency range of 10^{-1}–10^5 Hz was considered.

DC dielectric BDS measurements were performed by immersing the sample in silicone oil between vertically opposed ball bearings, 6.3 mm in diameter, and ramping the voltage at 350 V/s. The results were analysed using Weibull statistics within the Origin software using 90% confidence limits.

The DC current was measured for 1000 s at an applied field of 5 and 14.3 kV/mm, using a Keithley Instruments test fixture 8009 and picoameter 6517B. Data were acquired at three different temperatures (50, 60 and 70°C) and nominal conductivity values were calculated from the final ten resistance readings.

The space charge behaviour was investigated using the pulsed electro-acoustic (PEA) system to induce an acoustic signal in the sample with a 600 V amplitude and a pulse width of 5 ns, using silicone oil to obtain a good acoustic signal between the sample and the electrode. The high voltage electrode and the ground electrode were comprised of a semiconducting composite (Semicon) and aluminium (Al), respectively. Samples of thickness
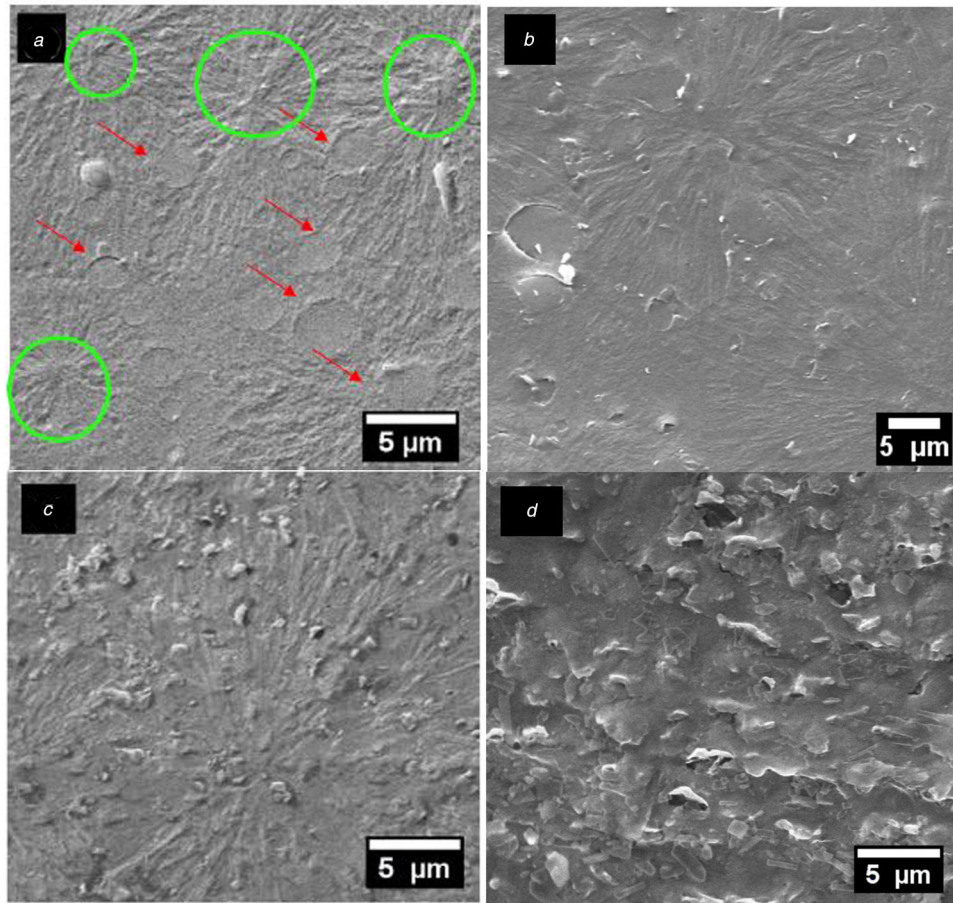
Fig. 1 *SEM micrographs of an etched internal edge of*
(a) PP/EVA/0, *(b)* PP/EVA/0.5, *(c)* PP/EVA/2.5, *(d)* PP/EVA/5. Green arrows highlight spherulites while red arrows highlight phase separation in Fig. 1a only

200 ± 5 μm were employed and the data were collected at room temperature for an hour under an applied electric field of +40 kV/mm, followed immediately with the short-circuit process (voltage-off) for an hour. The collected data were analysed by using LabVIEW. The net charge accumulation in the specimens was calculated according to (1), where $\rho(x)$ is space charge density, d is the thickness of a specimen, and S is the area of electrode

$$Q(t) = \int_0^d |\rho(x, t)| \cdot S \cdot \mathrm{d}x \qquad (1)$$

3 Results and discussion

3.1 Scanning electron microscopy

Fig. 1 shows a representative selection of SEM micrographs of etched, internal surfaces of the samples. The unfilled polymer blend in Fig. 1a shows significant phase separation and the PP shows significant spherulite formation. The phase separation is a result of the incompatibility between the PP and EVA and can be seen (highlighted by the red arrows) as circular distinct regions of different polymers; while spherulites are crystalline – highly ordered – regions of PP (highlighted by the green circles).

The organoclay can be seen in the other micrographs as flake-like structures. Although the etchant could remove some of the organic modifications to the organoclay (being polyolefin in nature [14]), the silicate layers of the clay should remain in position and still allow a representative SEM micrograph to be obtained. Taking the density of the organoclay in the composite to be between 0.2 and 0.5 g/cm^3 (valid given information from the manufacturer), together with published standard densities of the polymers and the compositional mixing ratios, the volume % of the filler can be calculated. For PP/EVA/0.5, PP/EVA/2.5, and PP/EVA/5, the volume % of the filler was calculated to be 0.9–2.2%, 4.5–10.6% and 8.9–19.6%, respectively. Although the density value used may

not be accurate, it serves to give a reasonable indication and can be checked against the SEM micrographs. The micrographs in Fig. 1 support these volume % values. It can be most clearly seen in Fig. 1d for PP/EVA/5, that viewing the micrographs in light of the volume % values allows the features seen to be interpreted as organoclay (and not as artefacts such as dust), which would not be intuitive when viewing the micrographs in terms of wt.% loadings alone.

The effect of the progressive addition of organoclay is clear in the polymer morphology and phase separation. Specifically, with the addition of organoclay, fewer and smaller spherulites are formed until, at 5 wt.% loading (shown in Fig. 1d), no spherulites or phase separation are observed. Along with this, phase separation is eliminated by loading of 2.5 wt.%. Clearly, the lowest organoclay loading investigated (0.5 wt.% in Fig. 1b) is insufficient to prevent phase separation and spherulite formation, whilst the 2.5 wt.% loading (Fig. 1c) can suppress the phase separation but not the spherulite formation. In the same way as work published on similar material systems, we attribute the suppression of both the phase separation and spherulite formation to the organoclay suppressing chain movement [15, 16]. These distinct changes to the sample morphology change with organoclay loading is notable and will be used to interpret the results from the dielectric investigations presented herein.

Differential scanning calorimetry was used to investigate the crystallinity/morphology change in the composite with organoclay loading but it was found that the results gave no relevant information and thus were omitted from this paper. Similarly, X-ray diffraction analysis was also used and the results have been published elsewhere [12].

3.2 Dielectric spectroscopy

Fig. 2 shows the dielectric spectroscopy data for all the composites and the unfilled polymer blend. In general, the sample without organoclay showed no change in the real permittivity with
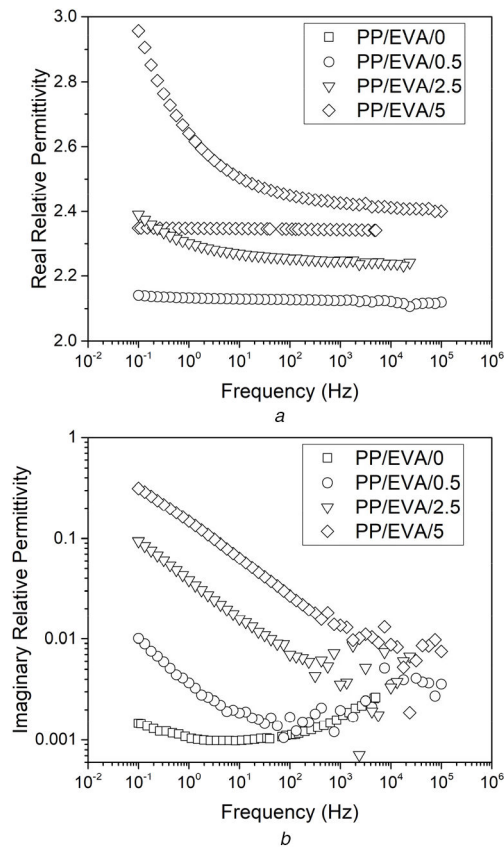
Fig. 2 *Dielectric spectroscopy results*
(a) Real and *(b)* Imaginary permittivity data
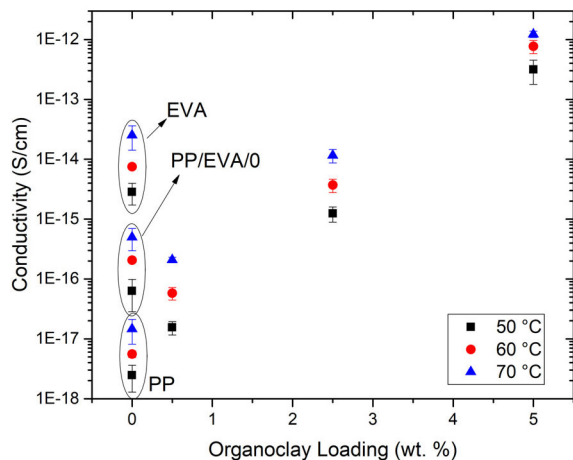
Fig. 3 *DC conductivity data measured under a field of 14.3 kV/mm. Each point represents the average (mean) result of three samples tested with the error being ± one standard deviation*

frequency whilst the nanocomposites show a loss beginning around 50 Hz. The imaginary permittivity of the unfilled blend was close to the system sensitivity limit, so the measurement was confirmed using a second analyser, which showed the same overall results. The results in Fig. 2. show that below 10^{-1} Hz, the imaginary permittivity increases with a decreasing frequency, which is in line with expectations. The composites showed a loss in the imaginary permittivity with a gradient of around –0.3 and an imaginary permittivity that increased with organoclay loading. Several points may be drawn out from these data. Firstly, the unfilled polymer blend, PP/EVA/0, has a permittivity value and independence from the frequency in line with the literature on PP [17], since PP makes up the majority of the sample, this result is as expected. Secondly, the organoclay increases the permittivity towards the lower frequencies in proportion to the filler loading amount. Since this loss is a result of Maxwell–Wagner interfacial polarisation between

the filler and the polymer and more filler will create more interfaces, this is entirely in line with expectations and has been seen elsewhere [18]. Finally, the gradient of the imaginary permittivity traces for the nanocomposites implies the loss at low frequencies is a result of both conduction and interfacial polarisation mechanisms [19, 20].

3.3 DC conductivity

DC conductivity measurements were made under fields of 5 and 14.3 kV/mm because the maximum voltage provided by the equipment was 1000 V and making thinner samples to compensate for this decreases the uniformity of the thickness and therefore the reliability of the results. Despite this field being on the low side for possible applications, we present these results as the principles and trends found should be true at higher fields as well.

Fig. 3 shows a summary of the DC conductivity data of the composites at two different temperatures. It can be seen that the organoclay changes the conductivity compared to the unfilled blend depending on the loading level. Together, these results suggest that the conductivity mechanism in PP/EVA/0 is dominated by the EVA and the effect of temperature is minimal in unfilled polymers. This is in contrast to the composites containing filler loadings above the percolation threshold (PP/EVA/2.5 and PP/EVA/5), which show a significant difference in conductivity with temperature. This suggests that the conduction mechanism is thermally activated [16] and is related to the proximity/overlapping of diffused charge clouds of the nanofiller facilitating charge transport [21]. The results for measurements taken under a field of 5 kV/mm reveal the same trend.

The results show that, for each respective temperature, the unfilled sample has a higher conductivity than the sample with the lowest organoclay loading level investigated. This is an interesting result, especially given that both PP/EVA/2.5 and PP/EVA/5 show considerable increases in conductivity with organoclay loading. This suggests that an organoclay loading level of 0.5 wt.% is not sufficient to form a percolating network and hence not able to create a morphology suitable for a percolating current. Given that the conductivity of a sample depends upon the local structure of the material, specifically the depth and positioning of the charge traps, which are influenced by the nanofiller, the co-continuity of the polymer phases and the extent of the crystalline and amorphous regions [22, 23], the observed morphology changes in Fig. 1 are significant to developing an understanding of these conductivity results. Specifically, the SEM results in Fig. 1 show that, of the nanocomposites, PP/EVA/0.5 had the most significant spherulite formation and was the only nanocomposite with phase separation. As such, we suggest that these are significant factors in determining the current flow through nanocomposites containing a conductive filler and immiscible polymers, as investigated herein.

Fig. 4 shows a selection of the current decay traces plotted on a log-log graph. The results show the effects of organoclay loading on the current – the higher the filler loading, the shorter the time until the decay plateaus. The results also show no significant difference at $t = 1000$ s between the unfilled polymer blend and the composite with the lowest organoclay loading, which is similar to the permittivity results data presented in Fig. 2. However, the similarities between PP/EVA/0 and PP/EVA/0.5 indicate that the same conduction mechanisms dominate. Specifically, conduction through the polymer, since percolation of the filler is not achieved at 0.5 wt.% loading.

Defining precisely the percolation threshold, we suggest, is of little gain to the literature as the value obtained would be specific to the polymers used, which are likely different to those used elsewhere and any application requiring the threshold being precisely known would need to conduct their own experiments with their materials and production methods. Herein, therefore, we only suggest the region that may be of interest to those investigating the percolation threshold of similar material systems (specifically 0.5–2.5 wt.%).
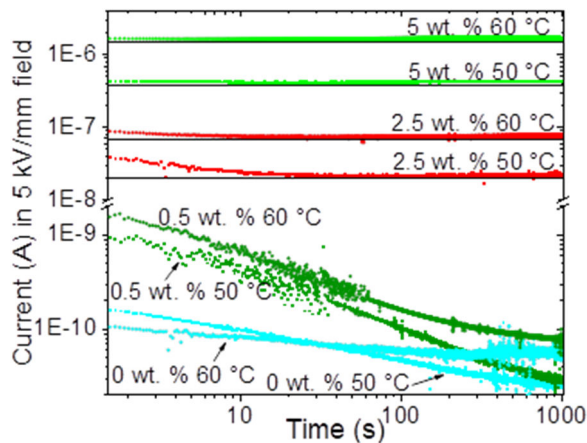
Fig. 4 *Log–log plot to assess the current decay of the samples under a field of 5 kV/mm, the PP/EVA/X – where X is labelled on the graph and the temperatures are also given. Horizontal lines have been added to aid inspection of the graph*
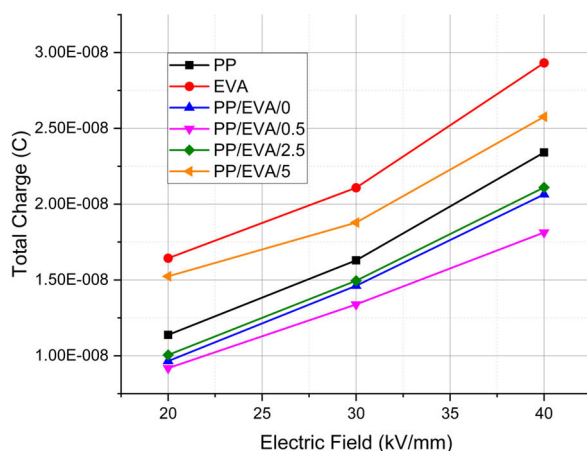
Fig. 5 *Graph comparing the charge accumulation after 1-hour of poling under different applied electric fields*

Table 1 Maximum field enhancement factor for all materials at 40 kV/mm

Sample	Maximum field enhancement, %
PP	10.0
EVA	17.5
PP/EVA/0	7.5
PP/EVA/0.5	5.0
PP/EVA/2.5	8.0
PP/EVA/5	25.0

3.4 Space charge

Fig. 5 shows the amount of charge accumulation after an hour poling under different applied electric fields. The blend of PP and EVA showed reduced the charge accumulation compared to pristine PP. Doping the blend with 0.5 wt.% of organoclay provided the lowest charge accumulation, while subsequent increases in filler content led to a proportional increase of charge accumulation. However, even at the highest loading of organoclay loading tested, 5 wt.%, the amount of charge accumulation is lower than in pure EVA. At higher organoclay loadings the percolation, i.e. the chances of overlap between neighbouring organoclay, increases, reducing the required hopping distances between neighbouring trap sites and, therefore, aid in the movement of charges [24, 25].

Comparing the charge accumulation of PP, PP/EVA/0, and PP/EVA/0.5, there is no significant difference under the lowest applied electric field of 20 kV/mm, with the difference being more pronounced at higher fields. Under the highest electric field applied

during testing, 40 kV/mm, the charge accumulation of PP/EVA/0.5 is significantly lower than in the PP/EVA/0 composite, indeed, lower than in any of the composites tested. We suggest this is a result of the clay acting as a multi-functional trap, able to capture and/or recombine charge carriers, as proposed by Tanaka [26, 27]. Under this higher field, charge carriers trapped at the interface or surface of the organoclay can obtain enough energy to overcome the potential energy barrier and move into the organoclay particle. This would trap charge carriers at the filler, which would act as recombination-centres under higher electric fields, leading to effective mitigation of observable space charge.

Space charge accumulation is known to cause electric field distortion in dielectrics. As a measure for such distortion, the field enhancement factor was calculated using (2), where E_{max} is the maximum electric field in the specimen and E_{DC} is the applied electric field. Results for the field enhancement factor are presented in Table 1

$$F_E = \frac{E_{max} - E_{DC}}{E_{DC}} \qquad (2)$$

The results confirm what could already be observed, that the blend of PP and EVA has a slightly lower electric field distortion compared with pristine PP. Most notably, the blend filled with the lowest organoclay content of 0.5 wt.%, can significantly reduce the electric field distortion, showing roughly half the field distortion found in pristine PP.
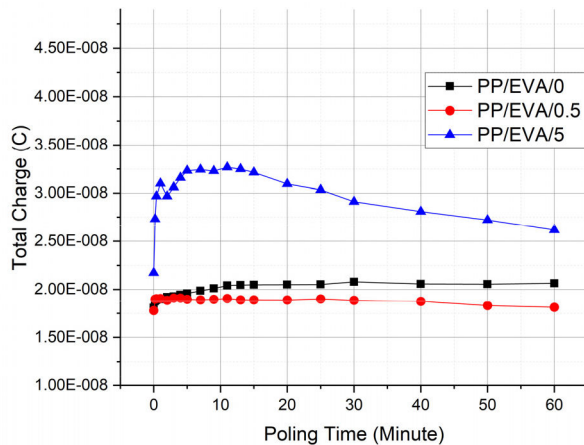
Fig. 6 shows the amount of charge accumulation in pristine PP and EVA under different applied fields. The accumulated charge in PP monotonically increased with poling time and is proportional to the applied electric field. In contrast to this, for the charge accumulation in EVA under the same conditions, a decrease in charge accumulation could be observed after an initial increase to a maximum value. This is especially notable under 40 kV/mm, where the amount of charge measured peaked initially, just to decrease significantly after 20 min of further poling. The reduction of charge accumulation in EVA is attributed to the saturation of EVA under a high electric field. Suzuoki *et al.* [28] stated that under high electric fields, the characteristics of conduction in EVA saturates because the charge transport velocity within the bulk is faster than the charge injection. The injected charge carriers move to the opposite electrode, rather than forming homocharge at the respective electrodes. Recombination of heterocharge can occur in the vicinity of the opposite electrode, but due to limitations in the spatial resolution and accuracy of PEA, it is difficult to pinpoint the precise location and rate of change. In EVA, positive charges tend to dominate the charge dynamics and are mobile, as outlined above. It is therefore likely that a recombination of charges at the cathode occurs after the charge moved through the bulk. The charge-carrier number density in the sample as well as the amount of injected charges can affect the recombination of charge carriers, hence this effect is more noticeable at higher electric fields.

It is clear that the charge accumulation in EVA is higher than in PP at the same applied electric fields. Many published papers have confirmed that the trapping states between the crystalline and amorphous regions of PP [29, 30] are mostly deep traps [31, 32]. The resulting carrier mobility within PP is therefore slow, indicating that charge carriers need much energy to de-trap once captured by the deep traps near the electrodes [30]. On the other hand, EVA has a higher amount of available shallow trapping sites. The existence of polar acetoxy groups can promote both positive and negative charge injections into the material, especially the higher positive charge [28]. The introduction of such a polar group is the main reason why EVA is dominated by large numbers of charge carriers. The injected charge carriers can easily move across the specimen, rather than being trapped near the electrode.

Fig. 7 shows the space charge accumulation under 40 kV/mm in PP/EVA/0, PP/EVA/0.5, and PP/EVA/5. The charge accumulation in PP/EVA/0 monotonically increases with the increasing polarisation time. The behaviour is analogous to pure PP shown in Fig. 6, only with slightly faster time to saturation. A lower overall charge accumulation can be observed in PP/EVA/0 than in pure PP and pure EVA, the latter showing a considerable decrease. The
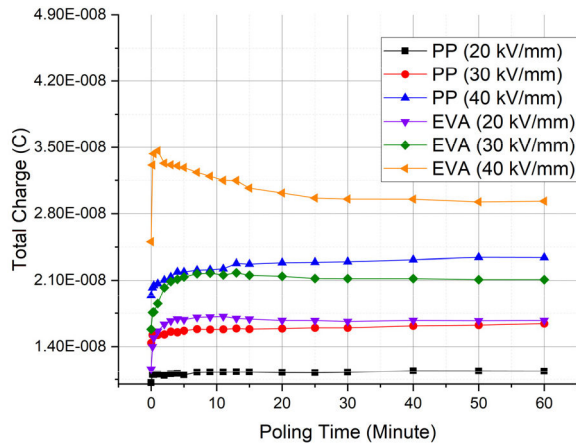
Fig. 6 *Space charge accumulation of PP and EVA under 20, 30, and 40 kV/mm*

Fig. 7 *Space charge accumulation of PP/EVA/0, PP/EVA/0.5 and PP/EVA/5 under a field of 40 kV/mm*

amount of charge accumulation in PP/EVA/0.5 changed in a similar fashion to PP/EVA/0. Moreover, the total charge accumulation after 1 h of poling in the PP/EVA/0.5 composite is the lowest of all the composites studied herein. In contrast, PP/EVA/5 samples showed significant charge accumulation, with a rapid increase at the beginning and a subsequent decrease with the increasing poling time. The amount of charge accumulation observed in PP/EVA/5 after 1 h of poling is higher than all of the specimens except for pure EVA. There is a slight reduction of space charge in PP/EVA/0.5 after 20 min poling time, but this is within measurement uncertainties. Quite significant is the reduction of charge accumulation due to higher charge mobility that can be observed in PP/EVA/5 samples. Charges can more easily move through the bulk than can be injected from the electrodes. The net effect is similar to EVA, as described above. The difference in behaviour depends upon the available defects in the specimen, meaning there are specific trapping sites that cause the easier recombination of charge carriers.

The space charge profile of the PP/EVA/0, PP/EVA/0.5, and PP/EVA/5 under 40 kV/mm are shown in Fig. 8. The unfilled polymer blend has heterocharge accumulation near both electrodes and distributed throughout the bulk area of the specimen. These heterocharges may be caused by ionisation dissipation under a high electric field, as a consequence of the existence of EVA in the specimen [28]. In other words, once there is enough energy to overcome the potential barrier, the charge carriers injected from the electrode can escape from trap sites by hopping to nearby unoccupied traps [33].

In contrast to this, the presence of organoclay causes a significant change: the charge dispersion and charge accumulation at the electrodes for PP/EVA/0.5 are lower than for PP/EVA/0. The lower distribution of charges should be related to the existence of

more trapping sites, inhibiting charge injection from the electrodes, which is caused by the organoclay. The consequence of the presence of more traps causes a reduction in the number of charges moving, from being the homocharges initially formed at both electrodes at the beginning of the poling time, towards accumulating as heterocharges at the cathode. This is because this field has a high enough energy that charge carriers can overcome the potential barrier. In doing so, the charge carriers can move to another unoccupied trapping site. However, the sample with the highest organoclay loading – PP/EVA/5 – shows homocharge accumulation in the vicinity of both electrodes immediately after the application of the DC voltage. With increasing poling time, the positive charges are formed at the cathode as heterocharges, while the peak of positive charges near the anode decreases. Most of the positive charges are formed within the central area of the specimen and the peak of positive charges is moved to the central area of the sample during the poling time. The greater dispersion of charge is due to the expansion of the interface region at higher organoclay loadings, caused by an overlap between neighbouring organoclay particles. The smallest distances between trapping sites of all the composites studied herein are in PP/EVA/5 since it has the highest organoclay loading. Therefore, the transport of trapped charges into empty traps is easiest in this composite.

### 3.5 DC dielectric breakdown strength

Fig. 9 contains the Weibull distributions of the dielectric BDS results, while the parameters are given in Table 2. Although compared to pure PP, the BDS decreased with the addition of EVA and organoclay, there is no statistical difference observed between the unfilled polymer blend, pure PP and the sample with the lowest filler loading. This is promising since the high BDS of PP is a key advantage to using this polymer and compromising the BDS is undesirable. This result may be attributed to the morphology being similar (see Fig. 1) and the organoclay loading being too low to increase the conductivity unlike the other composites (shown in Fig. 3).

Furthermore, the observation that increasing organoclay loading decreases the BDS aligns well with the literature for organoclay, silica, oxide and nitride-based nanofillers [16, 34, 35]. Possible mechanisms for this occurrence relate to the thermal instability of the material due to the clay increasing the sample conductivity, a higher current making an avalanche to breakdown more likely, space charge accumulation over ~2 min BDS measurement and/or the electric field enhancement due to agglomerations, specifically at higher filler loadings [5, 16, 34]. No matter the exact mechanism, taking the system holistically, it is reasonable to assume that organoclay, not being a polymer, has a detrimental effect on the DC dielectric BDS because it disrupts the homogeneous polymer. The organoclay has different conduction properties to the polymer and where they interact at the particle/polymer-interface, weak-points are formed where breakdown could be initiated, which make premature breakdown much more likely.

Another trend in the BDS data can be seen in the β values given in Table 2: the β values increase, compared to pure PP, upon addition of EVA and increases further upon addition of organoclay. Clearly, this is caused by a more reproducible breakdown mechanism(s) and we suggest that an understanding can be proposed considering the SEM micrographs in Fig. 1. We propose that the change in β values is due to there being fewer spherulites (which create weak points at interfaces) present upon addition of EVA and organoclay. Further weak points are eliminated upon addition of organoclay as phase separation of the polymers is inhibited, whilst the decrease in the β value for the highest organoclay loading could be due to the initial benefit being off-set by the creation of too many polymer-organoclay interfaces acting as weak points.

4 Conclusion

This work set out to investigate whether a polymer blend of PP and EVA could be compatibilised using organoclay without offsetting this benefit with detrimental effects on the dielectric performance of the composites. The results have shown that, although the
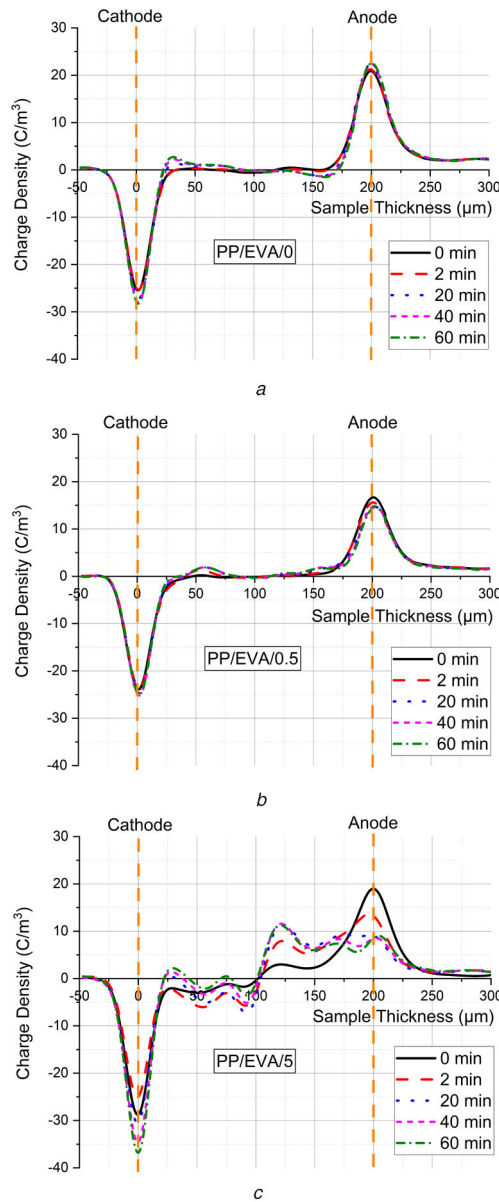
Fig. 8 *Space charge distributions under 40 kV/mm for*
(a) PP/EVA/0, (b) PP/EVA/0.5, and (c) PP/EVA/5
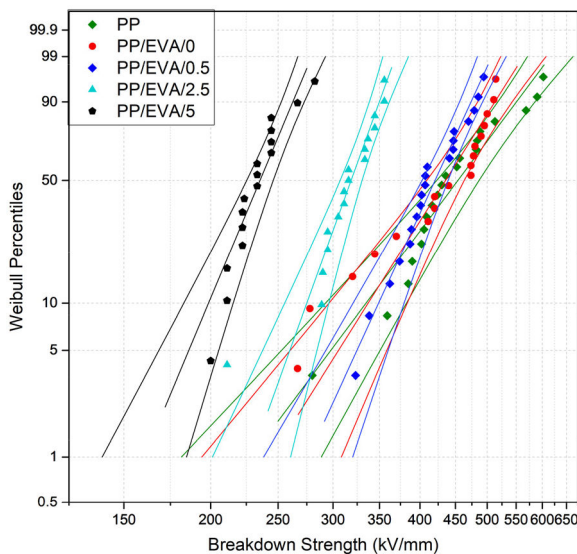
Fig. 9 *Weibull distributions of the DC dielectric BDS results*

Table 2 Summary of the Weibull distribution data calculated with 90% confidence limits

Sample	α, kV/mm	β
PP	481.4	6.2
PP/EVA/0	457.8	7.3
PP/EVA/0.5	436.2	10.1
PP/EVA/2.5	327.7	12.8
PP/EVA/5	243.4	11.0

influence of the filler on the dielectric properties can be minimised, the compatibilising ability cannot be preserved at such low loading levels. Despite this, compared to the unfilled system, and unlike the other nanocomposites, the sample with the lowest organoclay loading had:

- lower DC conductivity;
- an improved reproducibility of the breakdown tests (higher Weibull shape parameter);
- an insignificant effect on the scale parameter in the breakdown tests;
- an indistinguishable change in the real part of the complex permittivity, from 1 Hz to higher frequencies; and
- an insignificant amount of space charge.

This is a significant finding that makes it feasible to use otherwise incompatible polymer blends in high voltage electrical insulation without compromising their key dielectric properties, such as DC conductivity, BDS and permittivity. Furthermore, this work suggests that nanodielectrics with low filler loadings levels – one could say around the 'additive' level – could invoke better changes to a polymer than the typical filler loadings investigated in nanodielectric studies in literature. Specially, the results showed a clear difference in the dielectric performance of the materials, depending on whether the percolation point had been achieved. From these, we conclude that the percolation point is likely between 0.5 and 2.5 wt.% of organoclay loading in this polymer blend. Furthermore, we conclude the somewhat surprising result that using organoclay as an additive to immiscible polymer blends does not preclude these materials from HVDC applications.

5 Acknowledgments

6 References

[1] Cheewawuttipong, W., Fuoka, D., Tanoue, S*., et al.*: 'Thermal and mechanical properties of polypropylene/boron nitride composites', *Energy Procedia*, 2013, **34**, pp. 808–817

[2] Frounchi, M., Dadbin, S., Salehpour, Z*., et al.*: 'Gas barrier properties of PP/EPDM blend nanocomposites', *J. Memb. Sci.*, 2006, **282**, pp. 142–148

[3] Chen, H., Wang, W., Lin, Y*., et al.*: 'Morphology and mechanical property of binary and ternary polypropylene nanocomposites with nanoclay and CaCO3 particles', *J. Appl. Polym. Sci.*, 2007, **106**, pp. 3409–3416

[4] Eesaee, M., David, E., Demarquette, N.R.: 'Effect of blending and nanoclay on dielectric properties of polypropylene', *IEEE Trans. Dielectr. Electr. Insul.*, 2019, **26**, pp. 1487–1494

[5] Montanari, G.C., Fabiani, D., Palmieri, F*., et al.*: 'Modification of electrical properties and performance of EVA and PP insulation through nanostructure by organophilic silicates', *IEEE Trans. Dielectr. Electr. Insul.*, 2004, **11**, pp. 754–762

[6] Hosier, I.L., Vaughan, A.S., Swingler, S.G.: 'An investigation of the potential of ethylene vinyl acetate/polyethylene blends for use in recyclable high voltage cable insulation systems', *J. Mater. Sci.*, 2010, **45**, pp. 2747–2759

[7] Goodarzi, V., Jafari, S.H., Khonakdar, H.A*., et al.*: 'Morphology, rheology and dynamic mechanical properties of PP/EVA/clay nanocomposites', *J. Polym. Res.*, 2011, **18**, pp. 1829–1839

[8] Shaw, A.V, Vaughan, A.S., Andritsch, T.: 'Comparing the influence of organoclay on the morphology and dielectric properties of three thermoplastic polymers'. 2019 IEEE Conf. on Electrical Insulation and Dielectric Phenomena, Richland, WA, USA, 2019, pp. 46–49

[9] Goodarzi, V., Jafari, S.H., Khonakdar, H.A., *et al.*: 'An assessment of the role of morphology in thermal/thermo-oxidative degradation mechanism of PP/EVA/clay nanocomposites', *Polym. Degrad. Stab.*, 2010, **95**, pp. 859–869

[10] Martins, C.G., Larocca, N.M., Paul, D.R., *et al.*: 'Nanocomposites formed from polypropylene/EVA blends', *Polymer (Guildf).*, 2009, **50**, pp. 1743–1754

[11] Shafiee, M., Ahmad Ramazani, S.A., Danaei, M.: 'Investigation of the gas barrier properties of PP/clay nanocomposite films with EVA as a compatibiliser prepared by the melt intercalation method', *Polym. – Plast. Technol., Eng.*, 2010, **49**, pp. 991–995

[12] Shaw, A.V., Vaughan, A.S., Andritsch, T.: 'The dielectric properties of PP-EVA-organoclay composites'. 2019 IEEE Conf. on Electrical Insulation and Dielectric Phenomena. IEEE, Richland, WA, USA, 2019, pp. 42–45

[13] Shahin, M.M., Olley, R.H., Blissett, M.J.: 'Refinement of etching techniques to reveal lamellar profiles in polyethylene banded spherulites', *J. Polym. Sci. Part B Polym. Phys.*, 1999, **37**, pp. 2279–2286

[14] Olley, R.H., Bassett, D.C.: 'An improved permanganic etchant for polyolefines', *Polymer (Guildf).*, 1982, **23**, pp. 1707–1710

[15] Dong, Y., Bhattacharyya, D.: 'Investigation on the competing effects of clay dispersion and matrix plasticisation for polypropylene/clay nanocomposites. Part II: crystalline structure and thermo-mechanical behaviour', *J. Mater. Sci.*, 2012, **47**, pp. 4127–4137

[16] Eesaee, M., David, E., Demarquette, N.R., *et al.*: 'Electrical breakdown properties of clay-based LDPE blends and nanocomposites', *J. Nanomater.*, 2018, **2018**, article ID: 7921725

[17] Lide, D.R.: 'Dielectric constant of selected polymers', in Lide, D., *et al.* (Eds.): '*CRC handbook of chemistry and physics*' (CRC Press, Boca Raton, FL, USA, 2005), p. 2331

[18] Shaw, A.V., Vaughan, A.S., Andritsch, T.: 'The dielectric effect of xylene on an organoclay-containing composite', *IEEE Trans. Dielectr. Electr. Insul.*, 2019, **26**, pp. 890–897

[19] Tomer, V., Polizos, G., Randall, C.A., *et al.*: 'Polyethylene nanocomposite dielectrics: implications of nanofiller orientation on high field properties and energy storage', *J. Appl. Phys.*, 2011, **109**, pp. 074113-1–074113-11

[20] Pluta, M., Jeszka, J.K., Boiteux, G.: 'Polylactide/montmorillonite nanocomposites: structure, dielectric, viscoelastic and thermal properties', *Eur. Polym. J.*, 2007, **43**, pp. 2819–2835

[21] Abou-Dakka, M.: 'Evolution of space charges and conductivity with dc aging of polyethylene-synthetic and natural clay composites', *J. Nanomater.*, 2012, **2012**, pp. 1–8, doi:10.1155/2012/463748

[22] Li, S., Yang, L., Liu, W., *et al.*: '*Tailoring of nanocomposite dielectrics: from fundamentals to devices and applications; chapter 9. Tailoring of nanocomposite dielectrics*' (Pan Standford, Singapore, 2017), doi:10.1201/9781315201535-10

[23] Wang, Y., Mackernan, D., Cubero, D., *et al.*: 'Single electron states in polyethylene', *J. Chem. Phys.*, 2014, **140**, pp. 154902-1–154902-11

[24] Chen, G., Li, S., Zhong, L.: 'Space charge in nanodielectrics and its impact on electrical performance'. 2015 IEEE 11th Int. Conf. on the Properties and Applications of Dielectric Materials, Sydney, Australia, 2015, pp. 36–39

[25] Fothergill, J.C.: '*Dielectric polymer nanocomposites: electrical properties*' (Springer Science+Business Media, NY, USA, 2010), doi:10.1007/978-1-4419-1591-7_7

[26] Tanaka, T.: 'A quantum dot model for nanoparticles in polymer nanocomposites', *IEEE Trans. Dielectr. Electr. Insul.*, 2019, **26**, pp. 276–283

[27] Tanaka, T.: 'Roles of quantum dot like multi-functional traps in electrical conduction of polymer nanocomposites'. 1st Int. Conf. on Electrical Materials and Power Equipment, Xi'an, China, 2017, pp. 61–64

[28] Suzuoki, Y., Cai, G., Mizuntani, T., *et al.*: 'Effects of interface on electrical conduction in polyethylene-(ethylene-vinyl acetate) copolymer composites', *J. Phys. D Appl. Phys.*, 1984, **17**, pp. 141–146

[29] Zha, J.W., Yan, H.-D., Da, , *et al.*: 'Morphology and crystalline-phase-dependent electrical insulating properties in tailored polypropylene for HVDC cables', *Appl. Phys. Lett.*, 2016, **109**, pp. 222902-1–222902-5

[30] Zhou, Y., Hu, J., Dang, B., *et al.*: 'Titanium oxide nanoparticle increases shallow traps to suppress space charge accumulation in polypropylene dielectrics', *RSC Adv.*, 2016, **6**, pp. 48720–48727

[31] Zha, J., Wu, Y., Wang, S., *et al.*: 'Improvement of space charge suppression of polypropylene for potential application in HVDC cables', *IEEE Trans. Dielectr. Electr. Insul.*, 2016, **23**, pp. 2337–2343

[32] Yang, J., Gao, M., Zhao, H., *et al.*: 'Space charge characteristics of polypropylene modified by rare earth nucleating agent for β crystallization', *Materials (Basel).*, 2019, **12**, pp. 1–13

[33] Dissado, L.A., Fothergill, J.C.: '*Electrical degradation and breakdown in polymers*' (Institution of Engineering and Technology, London, UK, 2008), doi:10.1049/PBED009E

[34] Hosier, I.L., Praeger, M., Vaughan, A.S., *et al.*: 'The effects of hydration on the DC breakdown strength of polyethylene composites employing oxide and nitride fillers', *IEEE Trans. Dielectr. Electr. Insul.*, 2017, **24**, pp. 3073–3082

[35] Lau, K., Vaughan, A., Chen, G., *et al.*: 'On the space charge and DC breakdown behavior of polyethylene/silica nanocomposites', *IEEE Trans. Dielectr. Electr. Insul.*, 2014, **21**, pp. 340–351